Identification number: DOI : 10.1080/00221686.2012.753646
Official URL: http://dx.doi.org/10.1080/00221686.2012.753646

An experimental study on fish-friendly trashracks – Part 1. Inclined trashracks

SYLVAIN RAYNAL, PhD Student, *Axe HydEE (Hydrodynamique et Ecoulements Environnementaux), Institut P', CNRS – Université de Poitiers – ENSMA, UPR 3346, SP2MI – Téléport 2, 11 Boulevard Marie et Pierre Curie, BP 30179, 86962 Futuroscope Chasseneuil Cedex, France.*
Email: sylvain.raynal@univ-poitiers.fr (author for correspondence)

DOMINIQUE COURRET, Environmental Engineer, *Pôle Écohydraulique ONEMA – IMFT – IRSTEA, Institut de Mécanique des Fluides de Toulouse, 2 Allée du Professeur Camille Soula, 31400 Toulouse, France.*
Email: dcourret@imft.fr

LUDOVIC CHATELLIER, Assistant Professor, *Axe HydEE (Hydrodynamique et Ecoulements Environnementaux), Institut P', CNRS – Université de Poitiers – ENSMA, UPR 3346, SP2MI – Téléport 2, 11 Boulevard Marie et Pierre Curie, BP 30179, 86962 Futuroscope Chasseneuil Cedex, France.*
Email: ludovic.chatellier@univ-poitiers.fr

MICHEL LARINIER, Senior Environmental Engineer, *Pôle Écohydraulique ONEMA – IMFT – IRSTEA, Institut de Mécanique des Fluides de Toulouse, 2 Allée du Professeur Camille Soula, 31400 Toulouse, France.*
Email: larinier@imft.fr

LAURENT DAVID (IAHR Member), Professor, *Axe HydEE (Hydrodynamique et Ecoulements Environnementaux), Institut P', CNRS – Université de Poitiers – ENSMA, UPR 3346, SP2MI – Téléport 2, 11 Boulevard Marie et Pierre Curie, BP 30179, 86962 Futuroscope Chasseneuil Cedex, France.*
Email: laurent.david@univ-poitiers.fr

ABSTRACT
Experimental results are presented for trashracks placed in an open water channel with different bar shapes, spaces between bars and screen inclination angles. The numerous configurations provided results on head losses and on changes in velocity along the rack for a large range of situations, including fish-friendly trashracks. A new head-loss equation is proposed that takes into account the effect of the different tested parameters and demonstrates the need to separate the effect of the trashrack bars, which is directly related to the inclination of the trashrack, from the effect of the transversal elements such as spacer rows whose effect on the flow is not altered by rack inclination. Velocity measurements also adduce rules for efficient water intakes complying with fish-friendly criteria.

Keywords: Downstream migration; experimental hydraulics; head loss; inclined trashrack; open channel

1 Introduction

Fish mortality caused by turbines at hydroelectric plants during the downstream migration of fish is increasingly taken into account in Europe and particularly in France. After the restoration and protection plans for salmon (*Salmo salar*) and sea trout (*Salmo trutta*) in the 1990s, attention is now focused on the decline of European silver eel populations (*Anguilla anguilla*) (Travade and Larinier 2006, Travade *et al.* 2010). European Council regulation no. 1100/2007 established measures for the recovery of European eel stocks. It includes the requirement that all member states reduce anthropogenic mortality factors and notably the injuries inflicted on silver eels migrating downstream and passing through turbines. Mortality rates can be high because of the eels' elongated morphology (Monten 1985, Electric Power Research Institute 2001, Gomes and Larinier 2008). In addition, ecological continuity, including downstream migration of all species, has been identified as one of the hydromorphological

http://dx.doi.org/10.1080/00221686.2012.753646

elements which sustain the good ecological status of rivers, the goal of the European Water framework directive (2000/60/EC).

Fish-friendly turbines are one solution to address the downstream-migration issue, but they cannot be widely applied because they are efficient for limited head and discharge ranges. Interruptions in electrical generation during migration periods are another solution; however, it is not yet possible to predict migration periods accurately enough for cost-effective interruptions.

Consequently, transforming conventional intakes into fish-friendly ones is one of the most acceptable solutions. Fish-friendly intakes comprise a trashrack designed to guide fish towards its downstream end and to the entrances of bypasses, through which fish may avoid the turbines and safely reach the tailwater. Trashracks already exist on hydroelectric intakes to protect turbines from large debris. They are generally installed perpendicular to the flow, with 40–100 mm spaces between bars, and stop only the largest fish. To be considered fish-friendly, trashracks must have smaller clear spaces between bars to avoid the passage of fish through the turbines (less than 25 mm for salmon and sea trout smolts and less than 20 mm for silver eels) and should be inclined or angled to guide fish towards the bypasses located at the downstream end of the rack (Courret and Larinier 2008). Recommended values of inclination from the floor (β less than 25°) or of angle from the channel wall (α less than 45°) are based on the theoretical decomposition of the upstream velocity into normal and tangential components along the trashrack. To avoid impingement of smolts and silver eels on the rack, it is also recommended that the normal velocity V_n does not exceed 0.5 m s^{-1}. The implementation of these criteria generally induces drastic changes in the design of hydroelectric intakes.

Part 1 addresses inclined trashracks, ranging from conventional to fish-friendly configurations. It focuses on head losses, an important issue for hydroelectric operators, and on velocity distributions which influence the fish behaviour near the trashrack. In Part 2 (Raynal *et al.* 2012), the study addresses the second type of trashrack, i.e. angled trashracks.

Different equations have been proposed to calculate the head losses due to vertical and inclined trashracks. Kirschmer (1926) was one of the first authors to propose a head-loss equation for inclined trashracks with angles from $\beta = 90°$ (vertical) to $\beta = 60°$ (Eq. 1). His equation took into account the bar thickness b, the clear space between two bars e, the bar shape using the coefficient K_F and the screen inclination with $\sin(\beta)$ (illustration in Fig. 1).

$$\xi_{Kirschmer} = K_F \left(\frac{b}{e}\right)^{4/3} \sin(\beta) \qquad (1)$$

Since then, many researchers have attempted to improve the equation for vertical racks, for example, by taking into account transversal elements in the overall blockage ratio O_g defined as the ratio between the area of the immersed trashrack elements

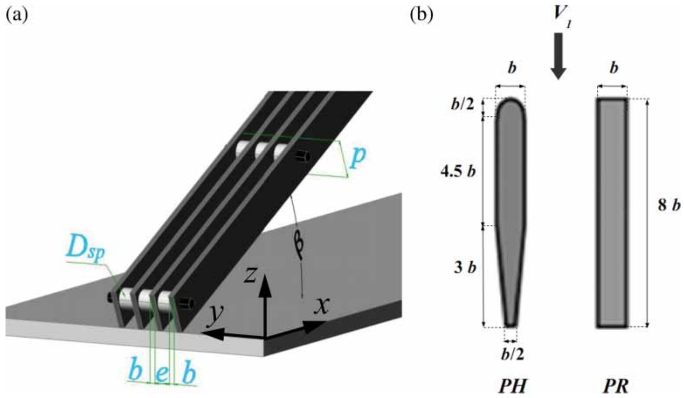

Figure 1 A trashrack with parameters and coordinates (a) and a focus on the different types of bar section (b) with dimensions (*PH* on the left and *PR* on the right)

and the whole trashrack area in the flow. Clark *et al.* (2010) determined that the trashrack head-loss coefficient (called ξ_{Clark} in Eq. 2) may be calculated as a function of O_g^2 which is equivalent in this case to $[b/(b+e)]^2$. This equation was obtained with blockage ratio O_g values between 37 and 8% (e/b ratio between 1.75 and 12, respectively). It also includes the bar shape with η (equal to 1 for rectangular bars).

$$\xi_{Clark} = 7.43\,\eta O_g^2 \qquad (2)$$

Osborn (1968) produced an equation for rectangular bars (Eq. 3 drawn from Clark and Tsikata 2009), which satisfied the boundary condition $\xi \rightarrow \infty$ when $O_g \rightarrow 1$

$$\xi_{Osborn} = \frac{O_g}{(1-O_g)^{7/3}} \qquad (3)$$

Meusburger *et al.* (2001) proposed an equation (Eq. 4) developed through experiments with vertical trashracks with blockage ratio O_g values between 55 and 19% (e/b ratio between 1 and 9, respectively). This equation included the effect of the bar depth p, but only one bar depth was tested

$$\xi_{Meusburger\ 2001} = K_F O_g^{1.33} \left(\frac{e}{p}\right)^{-0.43} \sin(\beta) \qquad (4)$$

Meusburger (2002) proposed a more general equation (Eq. 5), also applicable on angled screens and higher blockage ratio due to clogging (the corresponding terms do not appear in the following equation because they are equal to one for inclined screens), but where the effect of bar depth p was removed. This second equation satisfied the boundary condition $\xi \rightarrow \infty$ when $O_g \rightarrow 1$

$$\xi_{Meusburger\ 2002} = K_F \left(\frac{O_g}{1-O_g}\right)^{1.5} \sin(\beta) \qquad (5)$$

In both equations, Meusburger included the term $\sin(\beta)$ proposed by Kirschmer (1926) to take into account the rack inclination. However, he did not test any inclined racks and did not check its relevance. What is more, Meusburger studied the influence of each parameter separately and did not assess their possible interdependence.

Other authors carried out head-loss measurements in comparable configurations without systematically proposing head-loss equations, for instance, Tsikata *et al.* (2009a) who studied square and rounded bar profiles. In short, few equations for the design of inclined fish-friendly trashracks have been developed and the applicability of the equations quoted above has not necessarily been proven for vertical screens with very close bars, or for racks with low inclination angles.

An experimental investigation was carried out to check these equations and to extend them to trashracks with low inclination angles and narrow bar spacing. Based on a large range of configurations, the study also analysed the interdependence of the different parameters.

Characterization of flow velocities along the rack was also conducted to estimate the magnitude of currents likely to guide fish. In a similar manner, Tsikata *et al.* (2009b) measured velocities through vertical racks composed of a small number of bars using particle image velocimetry (PIV). However, they focused on the flow between and around bars, whereas the present study is more interested in the velocity distribution along the entire rack.

The second section describes the experimental set-up and presents the main characteristics of the hydraulic installation, the model trashrack and the different measurement devices. The third section focuses on head losses and provides a comparison of experimental results with the existing equations and proposes a new equation. The fourth section analyses the velocity profiles. These results are then discussed and recommendations are made for the design of fish-friendly water intakes with inclined trashracks.

2 Experimental set-up

The experiments were conducted with a model trashrack, in a 10-m long open channel that was 0.9 m deep and 0.6 m wide. A weir was installed at the outlet of the channel to adjust the water level. The upstream water depth H_1 was generally set to 0.3 m.

Trashracks were assembled with four main components. Components were scaled down to half size. Given a real bar 10 mm thick and 80 mm deep, the experimental bars were 5 mm thick (b) and 40 mm deep (p). This scale was adopted to maintain a ratio $H_1/b \geq 60$, which ensures that the drag coefficient of bars does not depend on water depth, according to Zimmermann (1969). It also made it possible to build trashracks with a large number of bars, at least 30 bars for the largest spacing tested. Bars were 1.3 m long (L_g) and had either a rectangular (PR) or a more hydrodynamic (PH) shape (Fig. 1). Six stainless-steel rods were inserted through all bars at a regular distance of 250 mm. Different spacers were installed around the rods. Their diameter (D_{sp}) was always 20 mm, while the space between bars (e) was set to 5, 7.5, 10 and 15 mm. These dimensions reproduced full-scale bar spacings between 10 and 30 mm and e/b ratios between 1 and 3. The two outer bars were 15 mm thick to attach the rack to the sides of the flume. All these elements determined the trashrack blockage ratio O_g, which may be broken down into two components, one representing the lateral blockage ratio O_b due to the bars and the other the blockage ratio O_{sp} due to the rows of spacers

$$O_g = O_b + O_{sp}$$
$$\text{with} \quad O_b = \frac{N_b b + 2b_{ext}}{B}, \quad O_{sp} = (1 - O_b)\frac{N_{sp,im} D_{sp}}{L_{g,im}} \tag{6}$$

where N_b, b, b_{ext}, B, $N_{sp,im}$, D_{sp} and $L_{g,im}$ are, respectively, the number of bars, the thickness of the bars, the thickness of the two outer bars, the width of the channel, the number of immersed spacer rows, the spacer diameter and the length of the immersed section of the trashrack. This last parameter was calculated as $L_{g,im} = H_1/\sin(\beta)$.

The foot of the model trashrack was attached so that the trashrack could rotate and be set to different inclinations (Fig. 1). Seven trashrack inclinations were tested, covering the most cases for actual hydraulic plants. The smallest angle was $\beta = 15°$ and the other angles were $\beta = 25$, 35, 45, 60, 75 and 90° (vertical trashrack).

Two main types of measurements were conducted. The flow rate Q, measured by an electromagnetic flowmeter, and upstream and downstream water depths (H_1 and H_2, respectively), measured with thin plates that were set flush with the free surface, allowed to calculate mean velocities ($V_{1,2} = Q/(BH_{1,2})$) and head losses. H_1 and H_2 were measured at $x = -1$ m and at $x = 2.6$ m, respectively ($x = 0$ m at the foot of the rack). The uncertainty of these water depths ranged between 0.5 and 1 mm, depending on the surface waves. Experiments without any screen were conducted to obtain the head loss due to the channel ΔH_0. The head losses exclusively due to the trashrack ΔH were determined subtracting ΔH_0 from the measured head losses, with a maximum overall uncertainty of 3 mm. Finally, the head-loss coefficient ξ was extracted from ΔH

$$H_1 + \frac{V_1^2}{2g} = H_2 + \frac{V_2^2}{2g} + \Delta H + \Delta H_0, \quad \Delta H = \xi \frac{V_1^2}{2g} \tag{7}$$

Velocity profiles were measured using two different instruments. First, a Sontek/YSI 16-MHz MicroADV (acoustic doppler velocimeter) was used to measure the three components of the local velocity in a cylindrical volume (6 mm wide and 9 mm high) with a 50 Hz sampling rate. Then, velocity profiles were measured along the trashrack using a 2D-traverse system. The second instrument was a PIV (Dantec Dynamic Studio) system (Fig. 2). The flow was seeded with 50 μm-diameter particles and illuminated with a laser sheet, perpendicular to the trashrack plane and emitted by a double-cavity Nd–YAG laser (Quantel 200 mJ, $\lambda = 532$ nm). Images were acquired at a rate of six double frames

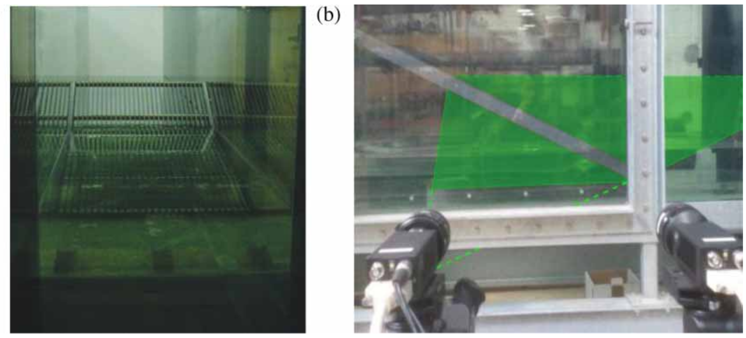

Figure 2 The inclined rack seen from inside the channel (a) and the PIV laser sheet (b) observed from near the cameras (emitted from the bottom)

per second by two 1600*1200 pixel dual-frame PIV cameras (JAI CV-M2). Dantec Dynamic Studio software was used to calculate the 2D particle movement between double frames with a region of interest (ROI) of approximately $24 \times 32\,\text{cm}^2$. About 75% of the water depth was contained in this ROI. The agitated-free surface of the water could reflect the laser sheet in any direction and eventually damage the CCD sensors of the cameras, which is why the free surface was excluded from the camera field to protect the cameras.

A total of 56 different experimental configurations were studied. Head losses were calculated and ADV measurements were made in all cases. PIV images were recorded for particular situations ($e = 10\,\text{mm}$; $\beta = 15, 25, 35$ or $45°$; rectangular and hydrodynamic shapes; laser sheet aligned with a bar or in between two bars).

3 Trashrack head-loss coefficient

3.1 *Invariance with regard to the Reynolds and Froude numbers*

The experiments were intended to be reproducible in real hydraulic plants. Because the study was carried out on a small-scale model with higher Froude numbers and lower Reynolds numbers than in real water intakes, preliminary tests were carried out to prove that the results obtained in our experiments could be extended to other Reynolds and Froude ranges. Equation (8) shows the R_b and F definitions used in this study. V_1 and H_1 are the upstream velocity and water depth, respectively, b the bar thickness, g the acceleration due to gravity and ν the kinematic viscosity

$$\mathsf{R}_\mathrm{b} = \frac{V_1 b}{\nu}, \quad \mathsf{F} = \frac{V_1}{\sqrt{g\,H_1}} \tag{8}$$

During the experiments, R_b and F were approximately 3000 and 0.4, respectively, whereas common values in real hydraulic plants are between 4000 and 13,000 for R_b and between 0.05 and 0.2 for F (calculated using real water-intake dimensions, drawn from Courret and Larinier 2008).

Preliminary experiments, with different flow rates, water depths and bar thicknesses (*PR* only), were also conducted in order to cover wider ranges of both the Reynolds and Froude numbers so that their influence on ξ could be determined.

Figure 3 shows some representative results concerning the behaviour of ξ with respect to R_b (model range for *PH*, model and actual range for *PR*) and F (model and actual range for both *PR* and *PH*). The large uncertainties observed for low R_b and F values correspond to measurements with low velocities and therefore to very low (millimetric) ΔH values. For each series, measurements showed that ξ remained roughly constant for a given trashrack configuration. It proved the applicability of the experimental results to real installations for rectangular bars. For profiled bars, the behaviour of ξ for full-scale R_b values had to be assumed on the basis of the behaviour of $\xi(\mathsf{R}_\mathrm{b})$ for rectangular bars.

3.2 *Experimental results*

Figure 4 shows the variation of measured head-loss coefficients ξ for the two bar shapes *PR* and *PH*, and different bar spacings, as a function of the rack inclination angle β. These two diagrams illustrate that ξ decreases with the decreasing inclination angle β and that it is generally lower for hydrodynamic bars than for rectangular ones. It also decreases when the clear spacing between bars increases.

In conclusion, the head-loss coefficient would seem to be dependent on the bar shape, the trashrack inclination angle β and its blockage ratio O_g, which is impacted by the bar spacing e, the bar thickness b, the number of immersed spacer rows $N_{sp,im}$ and their diameter D_{sp}.

3.3 *Empirical head-loss equation*

Before determining an equation for inclined trashracks, we first focused on vertical ones. Drawing on Meusburger's (2002) equation, Eq. (9) was proposed,

$$\xi_{\beta=90°} = K_i \left(\frac{O_g}{1 - O_g}\right)^M \tag{9}$$

in which K_i is either K_{PR} or K_{PH} depending on the bar shape.

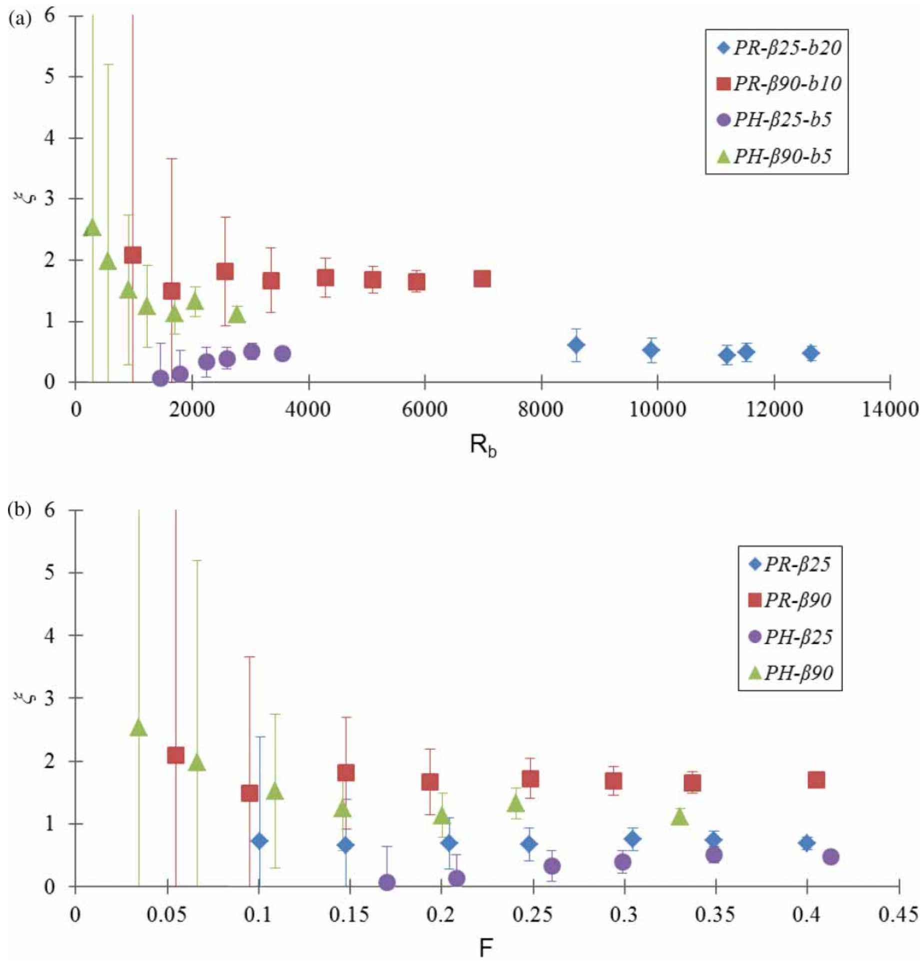

Figure 3 Variation of the trashrack head-loss coefficient ξ as a function of the R_b (a) and F (b) numbers. In the key to the figure, the bar shape, bar width (b = 5 mm if not stated otherwise) and trashrack inclination are indicated for each series. Points for which uncertainties exceed 100% correspond to configurations with low upstream velocity V_1

To fit the measured head-loss coefficients for vertical trashracks, we determined bar shape coefficients $K_{PR} = 2.89$ and $K_{PH} = 1.70$ for rectangular and hydrodynamic bars, respectively, and $M = 1.6$. Figure 5 compares, for a *PR* trashrack, the head-loss coefficient measured with predicted ones calculated with Eqs. (1–5) and (9). Except for the case where $e/b = 1$, the equations proposed by Osborn (1968), Meusburger *et al.* (2001), Meusburger (2002), and the one proposed here produced similar results. The Clark *et al.* (2010) equation produced good results for larger spaces between bars ($e/b > 2$), but did not perform well when applied to smaller spaces ($e/b < 2$). This is certainly due to the fact that their regression formula does not have the correct boundary condition when e tends to zero. Their experimental conditions (pressurized channel) may also partly explain these differences. The values of ξ calculated with the Kirschmer equation are too low. This may be explained by the fact that horizontal elements were not considered in the derivation of the equation.

Even if Eq. (9) matched our experimental results rather well for vertical racks, we could not adapt it to inclined racks, simply by adding a multiplicative term. Kirschmer (1926) indicated that, with β between 60 and 90°, the head loss of an inclined trashrack decreased by $\sin(\beta)$. However, multiplying Eq. (9) by $\sin(\beta)$ did not produce relevant results. A comparison between our measured points and different predicted coefficients for inclined trashracks, calculated with Eqs. (1), (4) and (5), is presented in Fig. 6. To highlight the effect of the inclination angle β, the curves were normalized to their respective $\xi(\beta = 90°)$ value obtained for vertical trashracks. At high inclination angles, the normalized head-loss coefficients $\xi/\xi(\beta = 90°)$ predicted by these three equations produced overestimated values. For low inclination angles, i.e. with more spacer rows immersed ($N_{sp,im}$ rises from 2 to 5, between $\beta = 90$ and 25°, respectively), the measured coefficients even tended to increase, which implies that they cannot be fitted using a standard sine shape.

An alternative approach could take into account the fact that the overall blockage ratio O_g does not represent very well the actual influence of each type of element constituting the trashrack, because bars and spacers have different geometries and orientations. Consequently, it appeared necessary to separate the effect of the trashrack bars which is directly related to the inclination of the trashrack and the effect of the transversal cylindrical spacers which depends on the number of immersed rows. It was proposed to calculate the blockage due to the transversal

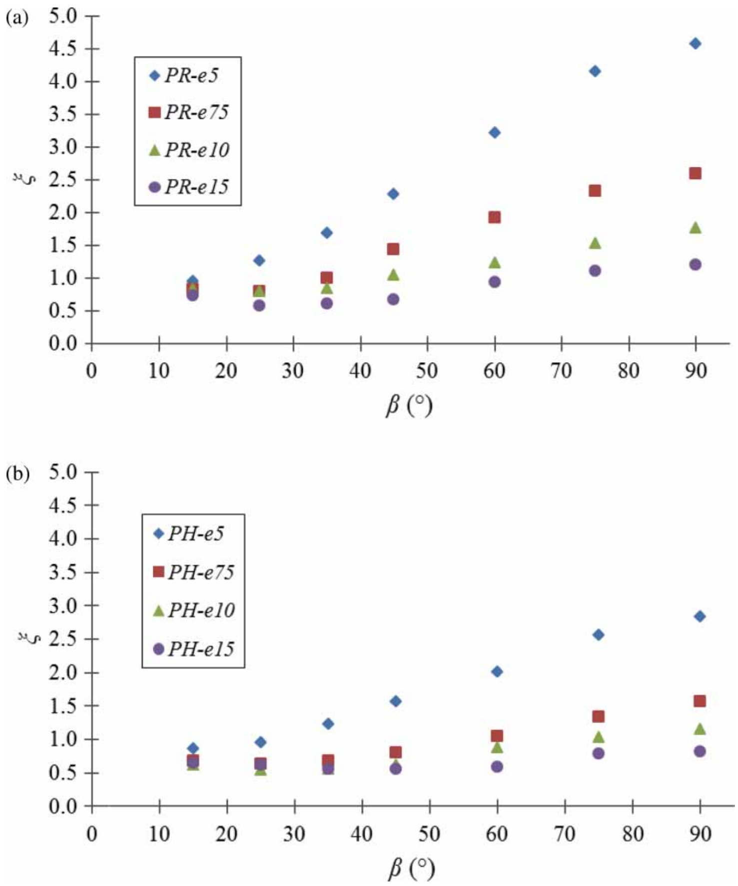

Figure 4 Variation of measured head-loss coefficients ξ for the two bar shapes PR (a) and PH (b), and different bar spacings (model dimension), as a function of the rack inclination angle β

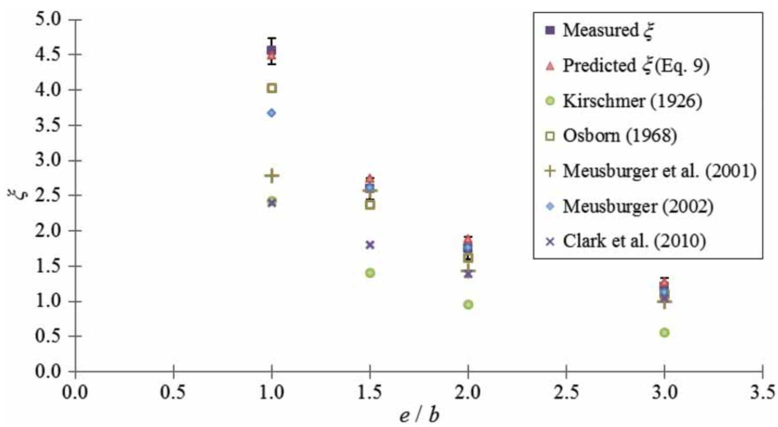

Figure 5 Comparison between the head-loss coefficients measured in this study for vertical rack and those calculated using the quoted equations (different e/b ratios and rectangular bars)

spacers relative to the channel cross-section rather than to the screen surface, yielding a blockage ratio $O_{sp,H}$ such that

$$O_{sp,H} = (1 - O_b)\frac{N_{sp,im} D_{sp}}{H_1} \tag{10}$$

This new variable makes it possible to separate the contributions of the vertical and horizontal elements. This led to testing the new equation.

$$\xi = A_i \left(\frac{O_b}{1 - O_b}\right)^{J_b} \sin^{J}(\beta) + C\left(\frac{O_{sp,H}}{1 - O_{sp,H}}\right)^{J_{sp}} \tag{11}$$

Five constants must be determined. A_i is a coefficient depending on the bar shape, C is a coefficient depending on the shape of transversal elements, whereas the three other coefficients should be constant. Adjustments using experimental results produced

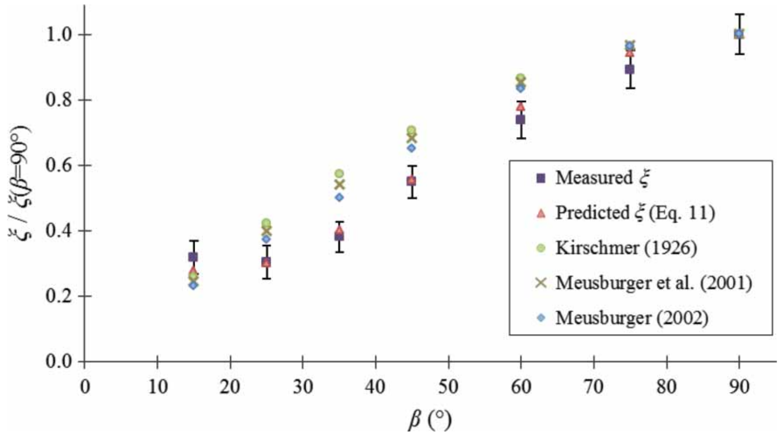

Figure 6 Comparison between the head-loss coefficient measured in this study for inclined racks and those calculated using the applicable equations (here rectangular bar $e = 7.5$ mm and $e/b = 1.5$). Each curve is rescaled using its head-loss coefficient for a vertical rack $\xi(\beta = 90°)$ to highlight the effect of the inclination angle β. In addition, the head-loss coefficient obtained with Eq. (11) is also shown

the following values:

$$A_{PR} = 3.85,\ A_{PH} = 2.10,\ C = 1.79,\ J = 2,$$
$$J_b = 1.65,\ J_{sp} = 0.77$$

Some points should be noted concerning these values:

- The constant A_{PH} for hydrodynamic bars is effectively lower than A_{PR} for rectangular bars.
- The value of C is equal to the shape coefficient of a cylinder determined by Kirschmer (1926).
- The exponent J_b, which equals 1.65, is quite close to the 1.5 of Meusburger.
- The influence of the blockage due to the bars seems to decrease by $\sin^2(\beta)$ instead of $\sin(\beta)$.

Head-loss coefficients calculated with Eq. (11) are plotted in Fig. 6. This equation was also tested on cases where some spacer rows were removed in order to check the influence of the terms representing the transversal elements in Eq. (11). The correlation coefficient, calculated for all the measured head-loss coefficients and those predicted by Eq. (11), was approximately 99.5%.

Despite the good correlation between Eq. (11) and our measurements, some questions concerning the influence of the geometrical parameters remain open. First, the position of transversal and vertical elements may modify some coefficients, especially those used as exponents J_b and J_{sp}. Given that the flow impacts the bars before the spacers, the flow reaching the spacers is not the same as the flow reaching the bars. It follows that a different position of the spacers on the bars could result in a different J_{sp} exponent. What is more, Eq. (11) has been validated for circular spacers. In real installations, the transversal elements can also be rectangular rods. As a result, the coefficient C should certainly be adapted to the shape of the transversal elements. This coefficient seems to be equivalent to the shape coefficient from Kirschmer (1926), whereas this is not the case for the bar shape coefficients A_{PR} and A_{PH}. This may be due to the proximity of bars which interfere with one another, while spacer lines seem to be distant enough not to influence each other.

4 Velocity distribution along an inclined trashrack

ADV and PIV techniques were used to acquire information about velocities near the rack in several different configurations. The two systems were used to carry out measurements in different but intersecting domains. The velocities measured at the intersection made it possible to compare ADV and PIV results. The results showed that both systems produced comparable data (less than 5% discrepancy, i.e. in the range of measurement uncertainties). Then, the two systems were combined. The PIV system produced a velocity map for each inclination (Fig. 7), whereas ADV was used to obtain the velocity profiles along the rack (Figs. 8 and 9). The laser sheet used for PIV, which was emitted in some cases from below the channel, crossed the screen and particularly the spacer lines. This degraded the correlations upstream of the rack and can be seen on some velocity maps (green lines upstream of the rack at $x = 500$ mm for $\beta = 15°$ in Fig. 7, for example).

From the velocity maps (Fig. 7), four observations can be mentioned.

- The flow velocity slightly increased at the foot of the rack ($x = 0$ m), just above the obstacle formed by the first spacer line.
- The acceleration along the rack was low and the velocity increase did not exceed 10%.
- The influence of the spacers on the upstream flow was strictly local.
- Even though the drag of the spacers had a large effect immediately downstream of the rack, this effect ceased further downstream. Streamlines quickly became parallel downstream of the spacers.

Breinig *et al.* (2003) performed a study on the velocity distribution along inclined racks composed of triangular bars. They

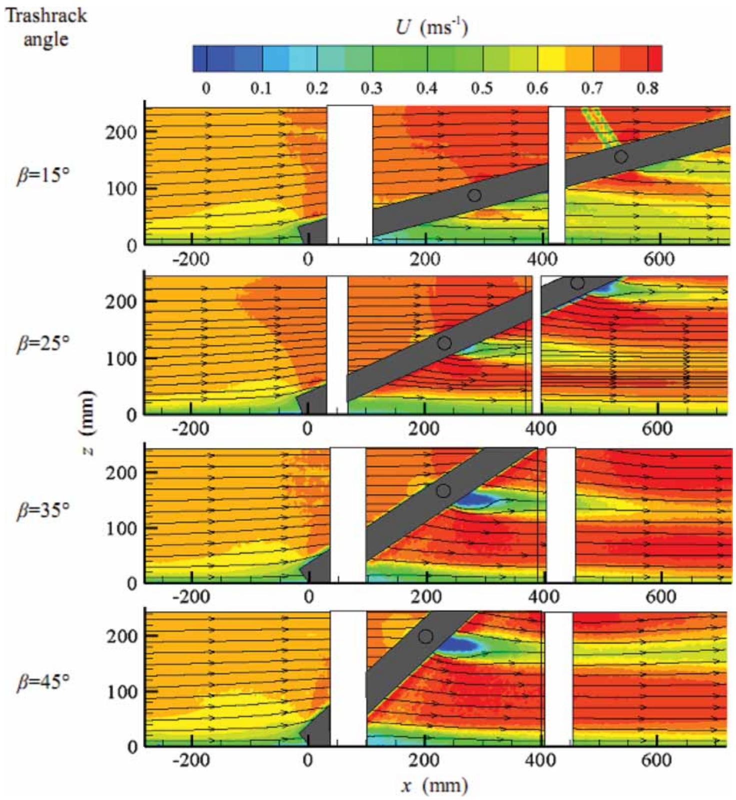

Figure 7 Velocity map (m s^{-1}) upstream and downstream of a trashrack inclined at different angles ($\beta = 15$, 25, 35 and 45°). $H_1 = 320$ mm. $V_1 = 0.67$ m s^{-1}

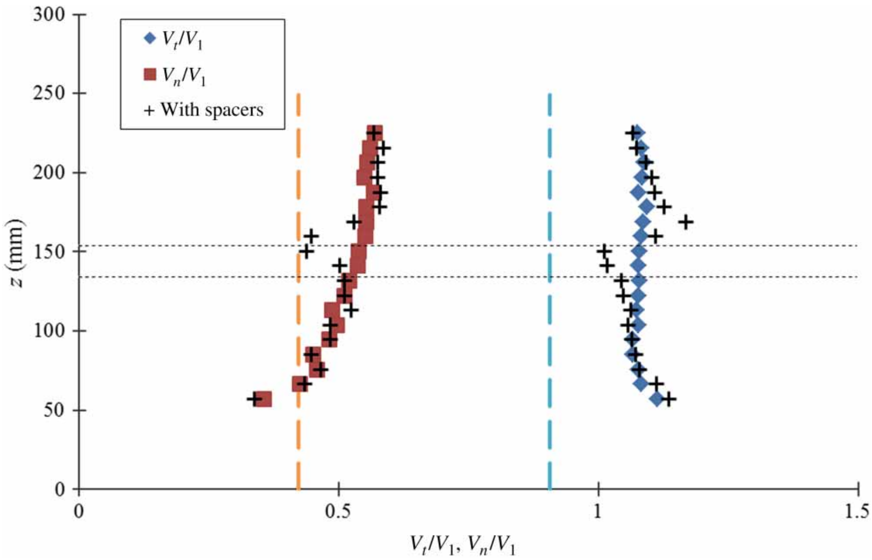

Figure 8 Comparison of normalized normal and tangential velocity profiles for a trashrack inclined at $\beta = 25°$, equipped with a spacer row (black marks) and without (colour marks). The horizontal dashed lines indicate the position and diameter of the spacer row. The vertical dashed lines represent the theoretical value of the normal (V_n/V_1) and tangential (V_t/V_1) velocities. $H_1 \approx 300$ mm

also observed that normal and tangential velocities were not significantly altered, noting that changes occurred mainly at low inclination angles (10% increase along the rack at $\beta = 15°$). Even though triangular bar screens are very different than those used for this study, our experimental results are comparable to the observations made by Breinig *et al.* (2003).

These qualitative results have been completed by quantitative results provided by the ADV measurements. Normal and tangential components of the velocity were measured along a profile running 20 mm from the bars. At this distance, the different configurations showed that neither the position of this profile (above a bar or between two bars) nor the bar shape had any influence on measured velocities. However, the spacer line had a very strong local impact.

Figure 8 shows the comparison of velocity profiles between a regular rack (black marks) and a rack from which spacer

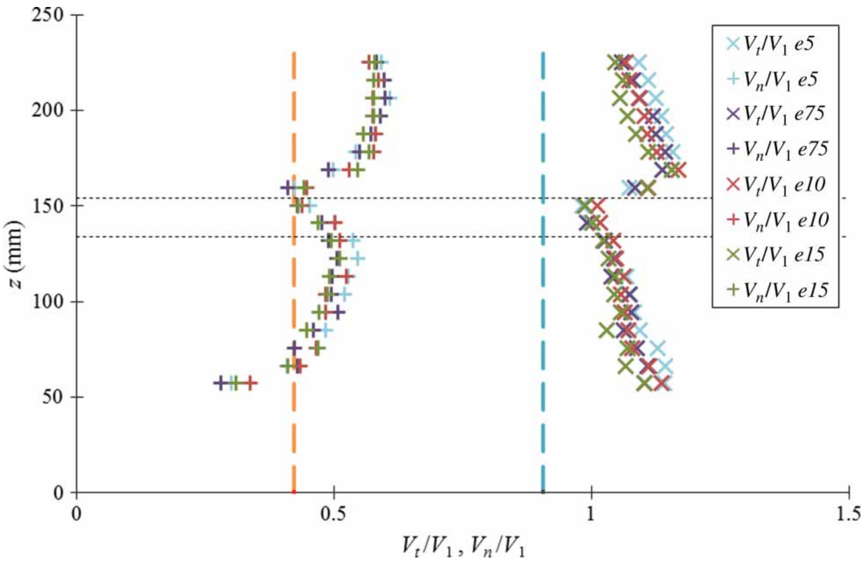

Figure 9 Normal and tangential velocity profiles along a trashrack inclined at $\beta = 25°$, for four different bar spacings ($e = 5$, 7.5, 10 and 15 mm). The horizontal dashed lines indicate the position and diameter of the spacer row. The vertical dashed lines represent the theoretical value of the normal (V_n/V_1) and tangential (V_t/V_1) velocities. $H_1 \approx 300$ mm

Table 1 Theoretical and measured values for V_t and V_n in the upper part of the rack ($z > 100$ mm or $z/H_1 > 0.3$)

	Theoretical values			Range of measured values (±10%)		
β (°)	$V_{t,theo}$	$V_{n,theo}$	$V_{t,theo}/V_{n,theo}$	V_t	V_n	V_t/V_n
15	0.97 V_1	0.26 V_1	3.73	1.20 V_1	0.35 V_1	3.35
25	0.91 V_1	0.42 V_1	2.14	1.05 V_1	0.55 V_1	2
35	0.82 V_1	0.57 V_1	1.43	0.95 V_1	0.70 V_1	1.4
45	0.71 V_1	0.71 V_1	1.00	0.80 V_1	0.85 V_1	0.9

Note: Measured velocities do not take into account the effect of spacers.

rows have been removed (colour marks). The bottom spacer line had to remain in place to maintain the rack in the correct position. The superposition of the curves indicates that the spacer rows had significant effects in a local zone, i.e. within a distance equal to two to three spacer diameters, but the vertical profile was not impacted beyond this zone. This means that the experimental velocity profiles were not significantly disturbed by the spacer rows and can be extrapolated to real installations.

One of the last questions was the influence of the clear bar spacing e on the velocity profiles. The blockage ratio O_g governs the ratio between the upstream velocity and the local velocity between the bars. ADV measurements were carried out to determine whether this local acceleration affects the upstream flow. Figure 9 compares the V_n and V_t profiles for four different bar spacings. The influence of e on V_n was very low and tended to be slightly higher for V_t. The difference between profiles *e5* and *e15* did not exceed 10%. This means that the bar spacing did not significantly modify the velocity profiles at a distance of four times the bar thickness from the rack (for e/b between 1 and 3).

The only way to notably modify the value of the tangential and normal components of the velocity is to change the inclination of the rack. By changing the axis of projection, V_n and V_t automatically change. However, velocities in Fig. 9 did not have the expected theoretical values (Table 1). The measured values of V_n and V_t in the upper zone of the flow ($z/H_1 > 0.3$) were approximately 30% higher than the values calculated by geometrical projection. The ratio between tangential velocity and normal velocity was slightly lower, but close to the theoretical values.

5 Conclusions

The effects of the trashrack bar spacing, shape and inclination on head losses and upstream velocity profiles were studied in a large number of configurations.

A head-loss equation (Eq. 11) was proposed covering both vertical and sharply inclined trashracks (low β). The head-loss coefficient was a function of the blockage ratios, the bar shape and the inclination of the rack. When trashracks were inclined, it appeared necessary to separate the blockage ratio due to bars (O_b) and the blockage ratio due to transversal elements such as spacer rows ($O_{sp,H}$). A comparison with detailed independent data could improve the validity of this equation.

The profiled bars improve the acceptability of trashracks with narrow bar spacing by diminishing the head loss due to the bars by 45%. However, the overall effect of the bar shape depends on the relative importance of blockage ratios O_b and $O_{sp,H}$, and therefore is likely to decrease with the inclination (lower β). In the experimental configurations, the gain with hydrodynamic bars was reduced to 20 and 10% for screen inclined at 25 and 15°, respectively.

The rack inclination is the only parameter that effectively changes the evolution of velocities along the rack. To incite fish to change their position in the water column and guide them to the downstream end of an inclined rack, where bypasses are located, it is recommended to generate a tangential component at least twice as large as the normal component (Courret and Larinier 2008). This study confirms that the rack must be sharply inclined to $\beta \leq 25°$ in order to satisfy this condition. For $\beta \leq 25°$, this study also shows that upstream mean velocities V_1 up to $1\,\mathrm{m\,s^{-1}}$ satisfy the condition on the normal velocity ($V_n \leq 0.5\,\mathrm{m\,s^{-1}}$) to avoid impingement of fish on the rack. As the approach velocities are often in the 0.6–0.9 $\mathrm{m\,s^{-1}}$ range in most water intakes, this should not be a limiting condition.

This study cannot yet provide information on how to position bypasses located at the downstream end of an inclined rack, with respect to the water intakes widths, nor on the required amount of flow in bypasses. A second study is underway for this purpose. However, a recommendation concerning the velocity V_b needed at the entrance of bypasses may already be suggested. Because the velocities must be as continuous as possible in order to attract fish, V_b should be close to the tangential velocity at the end of the rack, which means $V_b \approx 1.25\ V_1$.

This study produced experimental results transferable to real water intakes, on which practical recommendations may be based to comply with acknowledged biological constraints and to achieve fish-friendly intakes. Trashracks with low inclination angles and narrow spaces between bars would seem to be a particularly suitable solution because, considering the head loss, the influence of the small spacing is partly balanced by the rack inclination and the resulting increase of the screen area. One limit to this solution could be the length of the rack and the associated trashrakes, which rapidly increases with the rack inclination. Angled trashracks, which may avoid this problem, are studied in Part 2 (Raynal *et al.* 2012). Moreover, debris accumulation is increased in fish-friendly configurations due to the small spaces between bars, which raises questions concerning trashrake design.

Acknowledgements

This work was funded by the European Regional Development Fund (ERDF), the Région Poitou-Charentes, ONEMA, ADEME, CNR, SHEM and France Hydro-Electricité. Their support is greatly appreciated.

Notation

A_{PR}, A_{PH}	=	bar shape coefficient in Eq. (11) (–)
b, b_{ext}	=	bar thickness and thickness of the outer bars (m)
B	=	channel width (m)
C	=	shape coefficient of transversal elements in Eq. (11) (–)
D_{sp}	=	spacer diameter (m)
e	=	clear space between two bars (m)
F	=	Froude number (–)
g	=	gravitation acceleration ($\mathrm{ms^{-2}}$)
H_1, H_2	=	upstream and downstream water depths (m)
K_F	=	bar shape coefficient determined by Kirschmer (1926) (–)
K_{PR}, K_{PH}	=	bar shape coefficient in Eq. (9) (–)
J, J_b, J_{sp}	=	coefficients in Eq. (11) (–)
$L_g, L_{g,im}$	=	total and immersed bar lengths (m)
M	=	coefficient in the head-loss equation for vertical racks (–)
N_b	=	number of bars (–)
$N_{sp,im}$	=	number of immersed spacer rows (–)
η	=	bar shape coefficient determined by Clark *et al.* (2010) (–)
O_b	=	blockage ratio due to bars and outer bars (–)
O_g	=	blockage ratio (–)
$O_{sp}, O_{sp,H}$	=	blockage ratio of the transversal elements to the trashrack surface or to the upstream flow cross-sectional area (–)
p	=	bar depth (m)
PR, PH	=	bar shape (rectangular and hydrodynamic) (–)
Q	=	flow rate ($\mathrm{m^3\,s^{-1}}$)
R_b	=	bar Reynolds number (–)
U, V, W	=	velocity components along x, y and z, respectively ($\mathrm{m\,s^{-1}}$)
V_1, V_2	=	upstream and downstream mean velocities ($\mathrm{m\,s^{-1}}$)
V_t, V_n	=	components of the velocity tangential and normal to the rack face ($\mathrm{m\,s^{-1}}$)
V_b	=	bypass-entrance velocity ($\mathrm{m\,s^{-1}}$)
x, y, z	=	streamwise, transversal and vertical coordinates (m)
β	=	trashrack inclination angle from floor (°)
$\Delta H_0, \Delta H$	=	head loss due to the channel and head loss due to the rack (m)
λ	=	laser wavelength (m)
ν	=	kinematic viscosity ($\mathrm{m^2\,s^{-1}}$)
ξ	=	trashrack head-loss coefficient (–)

References

Breinig, T., Chorda, J., Larinier, M. (2003). Etude hydraulique de grilles Johnson® de faible porosité. Application à la dévalaison des larves de bichiques. *Report*, Rapport GHAAPPE RA03.02.

Clark, S., Tsikata, J. (2009). Effects of blockage ratio on energy loss through rectangular bar trashracks for hydro-turbines. Proc. 33rd *IAHR Congress*, Vancouver, Canada, 325–332.

Clark, S.P., Tsikata, J.M., Haresign, M. (2010). Experimental study of energy loss through submerged trashracks. *J. Hydraulic Res.* 48(1), 113–118.

Courret, D., Larinier, M. (2008). Guide pour la conception de prises d'eau 'ichtyocompatibles' pour les petites centrales hydroélectriques. Agence De l'Environnement et de la Maîtrise de l'Energie (ADEME) (www.onema.fr/IMG/pdf/2008_027.pdf).

Electric Power Research Institute (2001). Review and documentation of research and technologies on passage and protection of downstream migrating catadromous eels at hydroelectric facilities. *Report*, EPRI, Palo Alto, CA.

Gomes, P., Larinier, M. (2008). Dommages subis par les anguilles lors de leur passage au travers des turbines Kaplan – Etablissement de formules prédictives. *Report*, Rapport GHAAPPE RA08.05. Programme national de recherche-développement Anguilles-Ouvrages.

Kirschmer, O. (1926). Untersuchungen über den Gefällsverlust an Rechen, vol. 1. Mitteilungen des hydraulischen Instituts der TH München, Munich, Germany.

Meusburger, H. (2002). Energieverluste an Einlaufrechen von Flusskraftwerken. *PhD thesis*, Bau-Ing., ETH-Zürich (http://e-collection.library.ethz.ch/view/eth:26261).

Meusburger, H., Volkart, P., Minor, H.E. (2001). A new improved formula for calculating trashrack losses. Proc. 29th *IAHR Congress* Beijing, China, 804–809.

Monten, E. (1985). *Fish and turbines. Fish injuries during passage through power station turbines*. Vattenfall, Stockholm.

Osborn, J. (1968). Rectangular-bar trashrack and baffle headlosses, *J. Power Div.* 94(2), 111–123.

Raynal, S., Chatellier, L., Courret, D., Larinier, M., David, L. (2013). An experimental study in fish-friendly trashracks – Part 2. Angled trashracks. *J. Hydraulic Res*. 51(1), 67–75.

Travade, F., Larinier, M. (2006). French experience in downstream migration devices. Proc. Int. Conf. *International DWA symposium on water resources management*, Berlin. Hennef, Germany.

Travade, F., Larinier, M., Subra, S., Gomes, P., De-Oliveira, E. (2010). Behaviour and passage of European silver eels (*Anguilla anguilla*) at a small hydropower plant during their downstream migration. *Knowl. Manage. Aquatic Ecosyst*. 398(1), 1–19.

Tsikata, J.M., Katopodis, C., Tachie, M.F. (2009a). Experimental study of turbulent flow near model trashracks. *J. Hydraulic Res.* 47(2), 275–280.

Tsikata, J.M., Tachie, M.F., Katopodis, C. (2009b). Particle image velocimetry study of flow near trashrack models. *J. Hydraulic Eng.* 135(8), 671–684.

Zimmermann, J. (1969). Widerstand schräg angeströmter Rechengitter. Universität Fridericana Karlsruhe, Theodor-Rhebock-Flußbaulaboratorium, Mitteilungen Heft 157.